A Novel Synchronization Method in Terahertz Large-Scale Antenna Array System

Chinese Journal of Electronics
Vol.30, No.5, Sept. 2021

A Novel Synchronization Method in Terahertz Large-Scale Antenna Array System

ZHENG Chen[1], DING Xuhui[1], LIU Dekang[1], BU Xiangyuan[1] and AN Sining[2]

(1. *School of Information and Electronics, Beijing Institute of Technology, Beijing 100081, China*)

(2. *Microwave Electronics Laboratory, Department of Microtechnology and Nanoscience, Chalmers University of Technology, SE-41296 Gothenburg, Sweden*)

Abstract — We focus on the problems of the accurate time delay estimation, the design of training pilots, and hybrid matrix optimization within the large-scale antenna array Terahertz (THz) broadband communication system. In contrast to the existing researches based on narrow-band arrays, we hereby shed light on the time delay estimation of broadband arrays. In THz broadband communication systems, the data symbol duration is relatively short when comparing with the dimension of the antenna array. In large-scale antenna systems, signals received in each antenna are no longer different phase-shifted copies of the same symbol, but completely different symbols in which occasion traditional narrow-band structure is no longer suitable. Based on the above conclusion, firstly, we put forward a system model based on large-scale antenna arrays and Time delay line (TDL) structure. Secondly, we deduce the Cramer-Rao lower bound (CRLB) of the time delay estimation, and present a time delay estimation algorithm that could reach the CRLB. Thirdly, by minimizing the CRLB, we address the design of the training pilot and optimized TDL structure under the condition of constant envelope training pilot and modulus TDL structure. Finally, we disclose the numerical simulation results. According to the simulation results, the aforementioned method is workable in reaching the CRLB, the TDL structure can significantly surpass that of the traditional model, and the optimal pilot design method outperforms the pseudo-random pilot structure.

Key words — Large-scale antenna array, Time delay estimation, Constant modulus optimization, TDL structure.

I. Introduction

Multi-antenna array is a key technology that is capable of both making full use of spatial multiplexing and obtaining diversity gain in wireless communication systems[1–3]. It has been shown that future high-speed data networks need to rely on massive MIMO technology. Furthermore, for some special scenarios, the physical size constraints of the communication devices are no longer as strict as that in the cellular networks, allowing the size of the antenna arrays to become relatively larger. With the increasing requirements of channel capacity, the bandwidth of the traditional communication system can no longer meet the corresponding requirements[4,5]. Fortunately, the Terahertz (THz) technology enables us to utilize a larger bandwidth, a shorter wavelength, and a smaller antenna size, thus allowing us to carry more antennas in space-limited scenarios. Meanwhile, spatially dispersed users can be supported simultaneously due to the high-frequency band, weak signal scatters, and the channel's sparsity characters of the THz system.

Although the THz technology has so many advantages, some technical challenges still remain. Among them, synchronization is the core functionality of communication systems, especially for the THz high-speed communication system[6]. The large bandwidth characteristic of the signal makes it difficult for the Analog-digital-converters (ADCs) as well as Digital-analog-converters (DACs) to reach the Nyquist sampling rate while maintaining a high quantization bit number[7,8]. Furthermore, the accuracy of both ADCs and DACs deteriorates drastically at very high sampling rates, making it unsuitable for high-order modulation. Under this condition, only simple modulation methods, such as Binary-phase-shift-keying (BPSK) and On-off-keying (OOK) modulation types can be realized[9]. Meanwhile, extremely high accuracy in delay estimation is demanded due to ultrashort symbol duration. Compared with the Orthogonal-frequency-division-multiplexing (OFDM)

Manuscript Received Mar. 18, 2021; Accepted July 6, 2021. This work is supported by the National Natural Science Foundation of China (No.616220106001).

 DOI:10.1049/cje.2021.07.007

method, the accuracy of delay estimation in single-carrier modulation must be well within the interval of one sampling clock[10–12]. Basically, even tiny errors can significantly degrade the performance of the THz systems[13,14].

Generally, the output power of the THz amplifier is limited, and the THz signal attenuates more rapidly with distance. Therefore, to guarantee sufficient link margin, the corresponding antenna beamwidth should be narrow, which requires an extremely high Angle-of-arrival (AOA) estimation accuracy[15–17]. Under this condition, even a small azimuth angle error will cause a great loss of Signal-to-noise ratio (SNR) then destroy the quality of communication. Meanwhile, due to the real-time requirements of application scenarios, angle estimation needs to be completed in a very short time such as moving cars or Unmanned-Aerial-Vehicles that have a Line-of-sight (LoS) channel with users[18–20]. This undoubtedly requires a high-precision, high-speed estimation method[17,21–24].

For broadband array models, traditional research has focused on wideband DOA estimation and wideband beamforming to optimize the channel capacity. The corresponding method is to maximize the received SNR or minimizing the signal estimation variance[21,22]. However, in the broadband array, maximizing the SNR might not guarantee the optimal delay estimation accuracy. Furthermore, the huge computation complexity caused by the large array and wideband signal is another difficulty. To reduce the computational complexity, one solution is to simplify the complexity by using sparsity of angle, such as sparse array, analog matrix[25–30], and another method is to simplify the delay estimator by using sparsity of time delay, such as WMC structure[31–34]. A novel method named GAMP based compressed sensing recovery technology is an attracting interest[35–40]. However, the method based on compressed sensing inevitably has the problem of base mismatch, thereby a high-precision estimation method is necessary.

To cope with the above-mentioned challenges, this paper firstly presents a receiver structure model of constant modulus TDL for THz large-scale antenna array system. Using time-delay line technology and analog phase shifter technology, the problem of signal alignment on each antenna is solved by adjusting the phase of the phase shifter. Then, this paper deduces the Cramer-Rao bound (CRB) of time delay estimation under constant modulus TDL structure, and gives a time delay estimation method based on the spectrum structure of constant envelope signal, and proves that the estimation method can gradually reach the Cramer-Rao lower bound (CRLB). Then, aiming at minimizing the CRB, this paper gives the design method of training pilot and TDL structure under the condition of training pilot constant envelope and TDL structure constant modulus constraint. The numerical simulation results show that the estimation method can gradually reach the CRB; the proposed TDL structure can significantly surpass the traditional narrow-band array model; the optimal pilot design method is better than the pseudo-random pilot structure; even a small number of frequencies High-precision time delay estimation can be achieved.

The main contributions of this paper are listed as follows:

• This paper analyzes the reason that the traditional narrow-band large-scale antenna array structure is not suitable for THz communication, and establishes the system structure based on large-scale antenna array and TDL structure, and derives the spectrum structure of broadband receiving signal.

• The CRLB of time delay estimation under constant modulus TDL structure is derived, and a time delay estimation method based on the spectral structure of the constant envelope signal is presented. It is proved that the estimation method can gradually reach the Cramare boundary.

• The factors affecting the delay estimation in the communication system are demonstrated in our paper. Furthermore, the optimal design method under the constant modulus constraint of the training sequence as well as the optimal TDL structure is derived with the goal of minimizing the delay estimation of the CRLB.

The rest of this paper is organized as follows: Section II describes the system structure model of the THz large-scale antenna array and gives the received signal model. Section III derives the CRB based on the time delay estimation of the system model. An estimation method for progressively reaching the CRLB is given in this Section. In Section IV, the optimal training sequence design and optimal TDL matrix design methods are given with the goal of minimizing the CRB. Simulation results are given in Section V to evaluate the performance of proposed the algorithm. Conclusions can be found in Section VI.

II. System Structure and Signal Model

Due to the immature process of THz components, the output power is relatively small. In order to utilize the efficiency of the power amplifier at the transmitting end as much as possible, the constant envelope training pilot is used in this paper. The constant modulus phase coded training pilot containing I symbols is given by

$$x(t) = \sum_{i=0}^{I-1} x_i \cdot p(t - iT_f) \tag{1}$$

where $x_i = \rho e^{(\mathrm{j}\theta_i)}$ represents the i-th training symbol. To guarantee constant modulus, $\rho = 1$. $p(t)$ representing a shaped pulse for one symbol, could be chosen as a rectangular pulse, a root-raised-cosine pulse, or a Gaussian pulse. The duration of one symbol is T_f. The frequency-domain response of this pilot is given by

$$X(f) = FT\{x(t)\} = \sum_{i=0}^{I-1} x_i \cdot P(f) \cdot e^{\mathrm{j}2\pi f(i \cdot T_f)} \quad (2)$$

The THz channel response is $h(t-\tau)$, and the frequency response is $H(f)e^{\mathrm{j}2\pi f\tau}$, correspondingly. Specifically,

$$h(t) = F^{-1}\{H(f)\} \quad (3)$$

$$H(f) = \frac{c}{4\pi f d_T} \cdot \exp\left(-1/2K(f)d_T\right) \quad (4)$$

where $K(f)$ represents attenuation coefficient in THz frequency f. d_T represents the distance between the BS and the user. And τ represents the time delay from BS to the user, which we need to estimate. The signal received through the THz channel and its spectrum can be deduced as follows:

$$y(t) = \sum_{i=0}^{I-1} x_i \cdot g(t - iT_f - \tau) \quad (5)$$

$$Y(f) = \sum_{i=0}^{I-1} x_i \cdot G(f) \cdot e^{\mathrm{j}2\pi f(iT_f)} \cdot e^{\mathrm{j}2\pi f\tau} \quad (6)$$

Here, $g(t) = p(t) * h(t)$ represents the pulse after the shaped pulse passing through the THz channel. The Fourier transform is $G(f)$. Considering that the reflection of the THz signal is very weak in actual conditions, the power of such a multipath signal is much smaller than that of LOS. Therefore, only the signal of the direct path is considered in this paper. At the base station side, consider a line array receiver with M antennas. The interval between two adjacent antennas is d. Thereby the dimension of this antenna array is $(M-1)d$. For example, a THz communication system occupies center frequency $f_c = 150$GHz which wavelength $\lambda = c/f = 2$mm. The interval between two antennas is $d = \lambda/2 = 1$mm. So that, in a 128 antennas array, the size is $D = (M-1)d = 127$mm. Meanwhile, a signal with 10GHz symbol rate is transmitted, which duration $T_f = 100$ps. Then,

$$T_f \times c = 100\text{ps} \times 3 \times 10^8\text{m/s} = 30\text{mm} \leq 127\text{mm} \quad (7)$$

On such occasion, when the first symbol has just arrived at the No.0 antenna, the fifth symbol is already on the No.127 antenna, where existing narrowband assumption is no longer satisfied. At this time, each antenna is no longer a different phase-shifted copy of the same symbol, but a completely different symbol. In this case, we need to reintroduce the model of the received signal from the wideband array. Consider the signal arrived at m-th antenna is $y_m(t)$ with angle of arrival θ. $y_m(t)$ can be derived as follows:

$$y_m(t) = y(t - m\frac{d\sin\theta}{c}) \times e^{\mathrm{j}2\pi f_c m\frac{d\sin\theta}{c}} \quad (8)$$

Denote $\Delta\tau = \frac{d\sin\theta}{c}$ as the time delay between signal reached two adjacent antennas. We can get

$$\begin{aligned} y_m(t) &= y(t - m\Delta\tau) \\ &= \sum_{i=0}^{I-1} x_i \cdot g(t - iT_f - \tau - m\Delta\tau)e^{\mathrm{j}2\pi f_c m\Delta\tau} \end{aligned} \quad (9)$$

Correspondingly, we have

$$Y_m(f) = Y(f)e^{\mathrm{j}2\pi f m\Delta\tau}e^{\mathrm{j}2\pi f_c m\Delta\tau} \quad (10)$$

For the size $(M-1)d$ of the antenna array is much larger than the length $(T_f \times C)$ of a symbol propagating in space, so we employed an array receiver structure called a time delay line. Each antenna is followed by a set of time-delay lines (increased literature), each of which delays the signal by ΔT, and a series of delayed signals are summed by the digital phase shifter. Traditional TDL arrays require both digital phase shifters and digitally controlled attenuators to control the amplitude and phase of the signal. Intuitively, the time delay structure can align the signals on different antennas in time and then combine them, but this requires the coefficients of the TDL structure to have a two-dimensional adjustment of phase and amplitude, which is not suitable for large-scale antenna arrays. Therefore, in order to simplify the design, this paper uses a phase-shifting structure array to the only phase shift the signal delay. Due to the constant mode structure, it is not suitable for analysis in the time domain and needs to be considered from the frequency point of view.

Thus, the signal $r(t)$ passing through the TDL and digital phase shifters can be written as the summation of the M antenna branch signals after passing through the TDL structure.

$$r(t) = \sum_{m=0}^{M-1} r_m(t) \quad (11)$$

In which, $r_m(t)$ represents the summation of the signal received in the m-th antenna passing through TDL structure.

$$r_m(t) = \sum_{n=0}^{N-1} \left[y_m(t - n\Delta T) + n_m(t - n\Delta T)\right] w_{m,n} \quad (12)$$

Substitute $r_m(t)$ into the summation, we have

$$r(t) = \sum_{m=0}^{M-1}\sum_{n=0}^{N-1} y(t-m\Delta\tau-n\Delta T)e^{\mathrm{j}2\pi f_c m\Delta\tau}w_{m,n} + \sum_{m=0}^{M-1}\sum_{n=0}^{N-1} n_m(t-n\Delta T)w_{m,n} \quad (13)$$

Here, $R(f)$ is given by

$$R(f) = Y(f)\sum_{m=0}^{M-1}\left[e^{\mathrm{j}2\pi(fm\Delta\tau+fn\Delta T+f_c m\Delta\tau)}\right]w_{m,n} + \sum_{m=0}^{M-1} N_m(f)\left[e^{\mathrm{j}2\pi fn\Delta T}w_{m,n}\right] \quad (14)$$

The $r(t)$ is sampled in the time domain, with the sampling interval T_s, and the sampled signal $z(n)$. Its Fourier transform $Z(k)$ can be written in the following form.

$$\begin{aligned} z(n) =& r(nT_s) \\ =& \sum_{m=0}^{M-1}\sum_{n=0}^{N-1} y(nT_s-m\Delta\tau-n\Delta T)e^{\mathrm{j}2\pi f_c m\Delta\tau}w_{m,n} \\ &+ \sum_{m=0}^{M-1}\sum_{n=0}^{N-1} n_m(nT_s-n\Delta T)w_{m,n} \end{aligned} \quad (15)$$

$$\begin{aligned} Z(k) =& Y(f)\sum_{m=0}^{M-1}\sum_{n=0}^{N-1}\left[e^{\mathrm{j}2\pi(fm\Delta\tau+fn\Delta T+f_c m\Delta\tau)}\right]w_{m,n} \\ &+ \sum_{m=0}^{M-1} N_m(f)\left[e^{\mathrm{j}2\pi fn\Delta T}w_{m,n}\right] \\ =& Y(f_k)Tr(\boldsymbol{E}(f_k)\boldsymbol{W}^T) + \boldsymbol{n}(f_k)^T\boldsymbol{W}\boldsymbol{e}_n(f_k) \end{aligned} \quad (16)$$

In which,

$$\boldsymbol{E}(f_k)_{m,n} = \left[e^{\mathrm{j}2\pi(fm\Delta\tau+fn\Delta T+f_c m\Delta\tau)}\right] \quad (17)$$

$$\boldsymbol{e}_n(f_k) = \left[e^{\mathrm{j}2\pi f(0)\Delta T},\ldots,e^{j2\pi f(N-1)\Delta T}\right]^{\mathrm{T}} \quad (18)$$

$$\boldsymbol{n}(f_k) = [N_0(f_k),\ldots,N_{M-1}(f_k)]^{\mathrm{T}} \quad (19)$$

The essence of TDL is the weighted summation of the $M\times N$ different delayed signals $y(t-m\Delta\tau-n\Delta T)$ of the received signal $y(t-\tau)$. In this paper, to reduce the system cost, the entire TDL array finally synthesizes a signal $r(t)$ corresponding to one RF link. For the sake of generality, it is considered to increase the number of RF links, that is, both the digital-analog mixing and the TDL structure.

III. Near CRLB Estimation Method of Time Delay

According to the expression form of $Z(k)$, it can be seen that the spectrum of the received signal contains the following components:

$$\begin{aligned} Z(k) =& X(f_k)H(f_k)e^{\mathrm{j}2\pi f_k\tau}\times Tr(\boldsymbol{E}(f_k)\boldsymbol{W}^{\mathrm{T}}) \\ &+ \boldsymbol{n}(f_k)^{\mathrm{T}}\boldsymbol{W}\boldsymbol{e}_n(f_k) \\ =& \left[\sum_{i=0}^{I-1} x_i G(f_k)e^{\mathrm{j}2\pi f(iT_f)}\right]e^{\mathrm{j}2\pi f_k\tau} \\ &\times \sum_{m=0}^{M-1}\sum_{n=0}^{N-1}\left[e^{\mathrm{j}2\pi(fm\Delta\tau+fn\Delta T+f_c m\Delta\tau)}\right]\times w_{m,n} \\ &+ \sum_{m=0}^{M-1} N_m(f)\left[e^{\mathrm{j}2\pi fn\Delta T}\times w_{m,n}\right] \end{aligned} \quad (20)$$

- Training pilot: $X(f_k)=\sum_{i=0}^{I-1}x_i G(f_k)e^{\mathrm{j}2\pi f(iT_f)}$.
- Time delay need to be estimated: $e^{\mathrm{j}2\pi f_k\tau}$.
- Angle of Arriva: 1 $e^{\mathrm{j}2\pi fm\Delta\tau}e^{\mathrm{j}2\pi f_c m\Delta\tau}$. $e^{\mathrm{j}2\pi fm\Delta\tau}$ is caused by the too-short duration of a pulse, which is the most difference between traditional narrowband arrays. $e^{\mathrm{j}2\pi f_c m\Delta\tau}$ is caused by the center frequency, which is the same as the traditional narrowband array.
- Time delay line $e^{\mathrm{j}2\pi fn\Delta T}$. This is unique in TDL. Different from existing analog-digital hybrid array, thanks to this item, signals from different antennas can be aligned in time domain.
- Phase shifter matrix $w_{m,n}$. By properly designing this matrix, signals can be summed in phase, which could increase receiving signal-noise-ratio.
- Frequency domain noise $n(f_k)$. because of the additive-white-gaussian-noise assumption, noises in M antenna with different frequencies are independent identically distributed.

Based on previous analysis, in view of broadband of signal and the huge dimension of arrays, for a specific $\Delta\tau$, $f_k m\Delta\tau$ could not be negligible, and $e^{\mathrm{j}2\pi f_k m\Delta\tau}$ can't be approximated by 1. Thus, we need to rewrite $Z(k)$ as follows:

$$Z(k) = X(f_k)\cdot A(f_k,\Delta\tau)\cdot e^{\mathrm{j}2\pi f_k\tau} + W(f_k) \quad (21)$$

In which, $A(f_k,\Delta\tau)$ represents the inference arise from space angle. $e^{\mathrm{j}2\pi f_k\tau}$ contains the time delay which we need to estimate. $A(f_k,\Delta\tau)$ is given by

$$A(f_k,\Delta\tau) = \sum_{m=0}^{M-1}\sum_{n=0}^{N-1}\left[e^{\mathrm{j}2\pi(fm\Delta\tau+fn\Delta T+f_c m\Delta\tau)}\right]w_{m,n} \quad (22)$$

There has been a lot of literature on broadband DOA estimation. In this case, we assume $\Delta\tau$ is known.

Thus $A(f_k, \Delta\tau)$ is known at the same time, and can be abbreviated to $A(f_k, \Delta\tau) = A(f_k)$. Now, we need to estimate τ.

$$Z(k) = X(f_k)A(f_k)e^{\mathrm{j}2\pi f_k\tau} + W(f_k) \tag{23}$$

From the expression of $Z(k)$, it can be seen clearly that under zero noise, $Z(k) = X(f_k)A(f_k)e^{\mathrm{j}2\pi f_k\tau}$. Estimation of time delay can be replaced by estimating phase of $Z(k)$ in different frequency. For a specific frequency f_k, we can find

$$\hat{\tau} = \frac{1}{2\pi f_k}\left(\angle Z(k) - \angle X(f_k) - \angle A(f_K)\right) \tag{24}$$

In which, $X(f_k)$ and $A(f_k)$ can be calculated in advance. Accordingly, estimation of τ follows directly spectrum estimation of $Z(k)$. $Z(k)$ can be simply estimated by FFT or Wiener-Hopf method.

1. Deduction of CRLB

According the expression of signal, we could rewrite it in the following form

$$\begin{aligned} Z(k) &= X(f_k)A(f_k)e^{\mathrm{j}2\pi f_k\tau} + W(f_k) \\ &= s(k;\tau) + n(k) \end{aligned} \tag{25}$$

In which, $s(k;\tau) = X(f_k)A(f_k)e^{\mathrm{j}2\pi f_k\tau}$. Then we have the likehood function of received signal

$$\begin{aligned} &p(Z;\tau) \\ &= \prod_{k=0}^{K-1}\left[\frac{1}{\sqrt{2\pi\sigma_k^2}}\exp\{-\frac{1}{2\sigma_k^2}\left(Z(k) - s(k;\tau)\right)^2\}\right] \end{aligned} \tag{26}$$

By derivation and performing expectation, we can get

$$E\left(\frac{\partial ln(p(Z;\tau))}{\partial\tau}\right) = -\sum_{k=0}^{K-1} -\frac{1}{\sigma_k^2}\left(\frac{\partial s(k;\tau)}{\partial\tau}\right)^2 \tag{27}$$

Thus,

$$var(\hat{\tau}) \geq \left[\sum_{k=0}^{K-1} -\frac{1}{\sigma_k^2}\left(\frac{\partial s(k;\tau)}{\partial\tau}\right)^2\right]^{-1} \tag{28}$$

Further, we perform derivation to $s(k;\tau)$

$$\begin{aligned} \frac{\partial s(k;\tau)}{\partial\tau} &= \frac{\partial\left[X(f_k)A(f_k)e^{\mathrm{j}2\pi f_k\tau}\right]}{\partial\tau} \\ &= (j2\pi f_k)X(f_k)A(f_k)e^{\mathrm{j}2\pi f_k\tau} \end{aligned} \tag{29}$$

Substituting this result into (), we could have CRLB as follows

$$\begin{aligned} var(\hat{\tau}) &\geq \left[\sum_{k=0}^{K-1} -\frac{1}{\sigma_k^2}\left(\frac{\partial s(k;\tau)}{\partial\tau}\right)^2\right]^{-1} \\ &= \left[\sum_{k=0}^{K-1} -\frac{1}{\sigma_k^2}\|(\mathrm{j}2\pi f_k)X(f_k)A(f_k)e^{\mathrm{j}2\pi f_k\tau}\|^2\right]^{-1} \\ &= \left(\sum_{k=0}^{K-1}(2\pi f_k)^2\frac{\|X(f_k)A(f_k)\|^2}{\sigma_k^2}\right)^{-1} \end{aligned} \tag{30}$$

2. Near CRLB estimation method

Consider a specific frequency f_k

$$Z(k) = X(f_k)A(f_k)e^{\mathrm{j}2\pi f_k\tau} + W(f_k) \tag{31}$$

Denote $\hat{\phi_k} = \angle Z(k)$ as the phase of signal in this frequency, denote $\phi = \angle\left[X(f_k)A(f_k)e^{\mathrm{j}2\pi f_k\tau}\right]$ as the phase of noiseless signal in this frequency. Thus we can have such equation

$$\hat{\phi_k} = \angle Z(k) = \arctan\left(\frac{|X(f_k)A(f_k)|\sin\phi + \epsilon_s}{|X(f_k)A(f_k)|\cos\phi + \epsilon_s}\right) \tag{32}$$

In which, ϵ_s and ϵ_c represent $\mathrm{Im}[W(f_k)]$ and $\mathrm{Re}[W(f_k)]$ correspondingly Therefore, we perform the first-order Taylor expansion on the above estimator, without loss of generality, the following results

$$\begin{aligned} \hat{\phi} &= \arctan\frac{\rho\sin\phi + \epsilon_s}{\rho\cos\phi + \epsilon_c} = g(\epsilon_s, \epsilon_c) \\ &\approx g(0,0) + \frac{\partial g(\epsilon_s,\epsilon_c)}{\epsilon_s} + \frac{\partial g(\epsilon_s,\epsilon_c)}{\epsilon_c} \\ &= \phi + \frac{\partial g(\epsilon_s,\epsilon_c)}{\epsilon_s} + \frac{\partial g(\epsilon_s,\epsilon_c)}{\epsilon_c} \end{aligned} \tag{33}$$

Known that the derivation of $\arctan(x)$ is $1/(1+x^2)$, we can have

$$\hat{\phi} \approx \phi + \frac{1}{\rho}\left(\cos\phi\right)\epsilon_s + \frac{1}{\rho}\left(\sin\phi\right)\epsilon_c \tag{34}$$

ϵ_s and ϵ_c are i.i.d, sharing same gaussian distribute $N(0,\sigma^2)$. Thus $(\cos\phi)\,\epsilon_s + (\sin\phi)\,\epsilon_c \sim N(0,\sigma^2)$. After all, we can prove that, under small noise $\hat{\phi} \approx \phi + \frac{1}{\rho}n$, in which $n \sim N(0,\sigma^2)$. Then for the specific frequency f_k, the estimation of phase can be expressed as follows:

$$\hat{\phi_k} \approx 2\pi f_k\tau + \angle X(f_k) + \angle A(f_k) + n(k) \tag{35}$$

In which, $n(k) \sim N\left(0, \frac{\sigma_k^2}{|X(f_k)A(f_k)|^2}\right)$ By the estimation

of phase in f_k, we can estimate τ_k

$$\hat{\tau}_k = \frac{\hat{\phi_k}}{2\pi f_k} - \frac{\angle X(k)}{2\pi f_k} - \frac{\angle A(k)}{2\pi f_k} \tag{36}$$

$$\hat{\tau}_k \sim N\left(\tau, \frac{1}{(2\pi f_k)^2}\frac{\sigma_k^2}{|X(f_k)A(f_k)|^2}\right) \tag{37}$$

The estimation of the time delay can be achieved using any one of the frequency components f_k. But by observation of $\hat{\tau}_k$ probability distribution, we find that for a higher frequency f_k, $\hat{\tau}_k$ has a bigger denominator $(2\pi f_k)^2$, which means a smaller variance of $\hat{\tau}_k$. This shows that at the same SNR, higher frequency components can provide a more accurate frequency estimation. It is easy to understand that the additional phase caused by the high-frequency components is more pronounced during the same time delay. However, in practical systems, to reduce the Nyquist sampling rate, the high-frequency components in the signal are usually suppressed, and the signal energy is mainly concentrated on the low-frequency components. Moreover, considering design errors in realistic systems, high-frequency component signals may be distorted due to group delay and dispersion effects. Therefore, the time delay estimation accuracy can be improved by appropriately selecting the frequency component f_k or by appropriately distributing the signal power on different frequency components. By estimating the time delay of the K frequency components separately, K estimates $\hat{\tau}_k$ are obtained. Then linearly combine the K estimates to get the final time delay estimation τ.

$$\hat{\tau} = \sum_{k=0}^{K-1} \alpha_k \hat{\tau_k} \tag{38}$$

To get an unbiased estimation, $\sum_{k=0}^{K-1} \alpha_k = 1$

$$\hat{\tau} \sim N\left(\tau, \sum_{k=0}^{K-1} \alpha_k^2 \frac{1}{(2\pi f_k)^2}\frac{\sigma_k^2}{|X(f_k)A(f_k)|^2}\right) \tag{39}$$

By minimizing variance, we have

$$\begin{aligned} \min_{\alpha_k} \quad & \sum_{k=0}^{K-1} \alpha_k^2 \frac{1}{(2\pi f_k)^2}\frac{\sigma_k^2}{|X(f_k)A(f_k)|^2} \\ \text{s.t.} \quad & \sum_{k=0}^{K-1} \alpha_k = 1 \end{aligned} \tag{40}$$

The minimum variance is

$$\left(\sum_{k=0}^{K-1} \frac{(2\pi f_k)^2 |X(f_k)A(f_k)|^2}{\sigma_k^2}\right)^{-1} \tag{41}$$

The minimum variance is consistent with CRLB.

IV. Training Design and Matrix Optimization

Pseudo-random signals are often used as training sequences in engineering. For example, a phase-encoded signal sampled in a radar, a binary pseudo-random sequence in GPS, and the like. Since the pseudo-random sequence has good autocorrelation, the receiver can determine the delay estimate based on the cross-correlation of the received signal with the local replica. However, on the one hand, the pseudo-random sequence itself does not guarantee optimal performance, usually a sequence generated by a structured algorithm, which is difficult to search through exhaustively; on the other hand, since the receiver usually uses matched filtering, signal delay The estimation accuracy is limited by the sampling rate of the ADC, and the matched filtering requires a large number of parallel addition and multiplication operations, and the computational overhead is extremely large. In traditional pseudo-random synchronization signals, the signal energy is mainly concentrated near the baseband, such as the common singular spectrum. According to our previous discussion, the baseband low-frequency signal can provide limited delay estimation accuracy. Therefore, we need to redesign the optimal synchronous waveform according to the CRLB form of the signal.

In addition to the pilot $X(f_k)$, the design of the TDL array coefficients will directly affect the structure of $A(f_k)$, which in turn affects the performance of the delay estimation, so we also need to optimize the TDL array coefficients. The TDL structure of the array is fixed, and needs to be optimized, which is the phase weighting coefficient $w_{m,n} = e^{\mathrm{j}\theta_{m,n}}$ after each stage delay. Wherein, the time delay structure of the array is fixed and needs to be optimized, that is, the phase weighting coefficient after each stage delay is different for the conventional narrowband array, because the different phase copies of the same data symbol are received on each antenna, therefore, the phase weighting coefficient is designed to adjust the phase of each signal so that the beam direction of the antenna is aligned with the angle of arrival. For wideband arrays, the symbols on the individual antennas are different because of the short duration of the data symbols and the large size of the antenna array. Thus, the basic idea of design $w_{m,n}$ is to align the originally unsynchronized symbols. An intuitive solution is to delay the signals received by the antennas in the time domain. However, this requires that both the amplitude and phase of $w_{m,n}$ can be adjusted. Another indirect solution is to understand the TDL structure behind the antenna as a filter. By adjusting the tap coefficients of the filter, the gain of different frequency points of the signal is changed, thereby improving the overall delay estimation accuracy.

Thus, based on the previous analysis, we designed the training sequence X and the TDL matrix W to minimize CRLB.

1. Training design

In a communication system, in order to ensure communication quality and maximize the signal to noise ratio of the received signal, the selection of W is usually fixed. So, we assume that W is known to optimize X. Recalling the previous derivation of the CRLB

$$CRLB = \left(\sum_{k=0}^{K-1} \frac{(2\pi f_k)^2 |X(f_k)A(f_k)|^2}{\sigma_k^2} \right)^{-1} \tag{42}$$

We rewrite the previous problem as follows:

$$\begin{aligned} \max_{x} \quad & \sum_{k=0}^{K-1} \frac{(2\pi f_k)^2 |X(f_k)A(f_k)|^2}{\sigma_k^2} \\ \text{s.t.} \quad & |x_i| = 1 \end{aligned} \tag{43}$$

Then we express it into detail

$$X(f_k)A(f_k) = G(f_k)[\boldsymbol{x}^{\mathrm{T}} \boldsymbol{F}(f_k)] Tr[\boldsymbol{E}(f_k)^{\mathrm{T}} \boldsymbol{W}] \tag{44}$$

and

$$\begin{aligned} \sigma_k^2 &= E\left[\left(\boldsymbol{n}(f_k)^{\mathrm{T}} \boldsymbol{W} \boldsymbol{e}_n(f_k) \right)^{\mathrm{H}} \left(\boldsymbol{n}(f_k)^{\mathrm{T}} \boldsymbol{W} \boldsymbol{e}_n(f_k) \right) \right] \\ &= \sigma_n^2 Tr\left[\boldsymbol{W} \boldsymbol{e}_n(f_k) \boldsymbol{e}_n(f_k)^{\mathrm{H}} \boldsymbol{W}^{\mathrm{H}} \right] \end{aligned} \tag{45}$$

Then, we have

$$\sum_{k=0}^{K-1} \frac{(2\pi f_k)^2 |X(f_k)A(f_k)|^2}{\sigma_k^2} = \boldsymbol{x}^{\mathrm{H}} \boldsymbol{\Sigma} \boldsymbol{x} \tag{46}$$

In which,

$$\boldsymbol{\Sigma} = \sum_{k=0}^{K-1} \left[(2\pi f_k)^2 \boldsymbol{F}(f_k) \boldsymbol{F}(f_k^H) \frac{|G(f_k) Tr[\boldsymbol{E}(f_k)^T \boldsymbol{W}]|^2}{\sigma_k^2} \right] \tag{47}$$

Therefore, the initial optimization can be converted into such formation

$$\max_{x} \quad \boldsymbol{x}^{\mathrm{H}} \boldsymbol{\Sigma} \boldsymbol{x} \tag{48}$$

$$\text{s.t.} \quad |x_i| = 1 \tag{49}$$

According to the form of the problem, the feature decomposition can be directly performed on $\boldsymbol{\Sigma}$.

$$\boldsymbol{\Sigma} = \boldsymbol{U} \boldsymbol{\Lambda}_X \boldsymbol{U}^{\mathrm{H}} \tag{50}$$

Denote u as the primitive eigenvector of $\boldsymbol{\Sigma}$. To satisfy the constant modulus constraint, we choose the phase of u as optimal x. Thus, the optimal pilot is given by

$$\boldsymbol{x}^{opt} = \exp(\mathrm{j} \cdot \angle \boldsymbol{u}) \tag{51}$$

2. TDL matrix optimization

For radar and other systems, the radar waveform is usually given. Here, the delay estimation is the most important part. Therefore, the W matrix of the TDL structure needs to be designed. We assume that the training sequence is fixed and only optimize for W. By observing the structure of the system, we can find that $e^{\mathrm{j}2\pi f n \Delta T}$ and $w_{m,n}$ together consist of a frequency selection structure, which changes the power corresponding to a different frequency, and thus changes the accuracy of time delay estimation using the line. Under the premise that the incident angle is known, by changing W, the gain of the array for different frequencies can be changed. Intuitively, for frequency $f_k = f_0$ the optimal choice of the coefficient is $w_{m,n}^{opt} = (e^{-\mathrm{j}2\pi f m \Delta\tau} e^{-\mathrm{j}2\pi f n \Delta T} e^{-\mathrm{j}2\pi f_c m \Delta\tau})$. While, for another frequency $f_k = f_1$, this optimal solution may not be applicable at all. So it is necessary to optimize the design. Similar to the design of the training sequence, we first rewrite the original problem.

$$\begin{aligned} \max_{W} \quad & \sum_{k=0}^{K-1} \frac{(2\pi f_k)^2 |X(f_k)A(f_k)|^2}{\sigma_k^2} \\ \text{s.t.} \quad & |w_{m,n}| = 1 \end{aligned} \tag{52}$$

Express the summation, and the numerator can be rewritten as follows:

$$\begin{aligned} & (2\pi f_k)^2 |X(f_k)A(f_k)|^2 \\ &= |X(f_k)|^2 \mathrm{Tr}\left[\boldsymbol{E}(f_k)^{\mathrm{T}} \boldsymbol{W} \right] \\ &= (2\pi f_k)^2 |X(f_k)|^2 \left(vec(\boldsymbol{E}(f_k))^{\mathrm{T}} vec(\boldsymbol{W}) \right)^2 \\ &= (2\pi f_k)^2 |X(f_k)|^2 \left(\boldsymbol{e}(f_k)^{\mathrm{T}} \boldsymbol{w} \right)^2 \\ &= (2\pi f_k)^2 |X(f_k)|^2 \left(\boldsymbol{w}^{\mathrm{H}} \boldsymbol{e}(f_k)^* \boldsymbol{e}(f_k)^{\mathrm{T}} \boldsymbol{w} \right) \\ &= \boldsymbol{w}^H \boldsymbol{\Sigma}_{XAE}(f_k) \boldsymbol{w} \end{aligned} \tag{53}$$

And the denominator can be expressed as

$$\begin{aligned} \sigma_k^2 &= \sigma_n^2 \mathrm{Tr}\left[\boldsymbol{W} \boldsymbol{e}_n(f_k) \boldsymbol{e}_n(f_k)^{\mathrm{H}} \boldsymbol{W}^{\mathrm{H}} \right] \\ &= \sigma_n^2 \boldsymbol{w}^{\mathrm{T}} \left[e_n(f_k) e_n(f_k)^{\mathrm{H}} \otimes I_{M \times M} \right] \boldsymbol{w}^* \\ &= \boldsymbol{w}^{\mathrm{H}} \boldsymbol{\Sigma}_{NE}(f_k) \boldsymbol{w} \end{aligned} \tag{54}$$

In which,

$$e_n(f_k) = \left[1, \ldots, e^{j2\pi f_k (N-1)\Delta T} \right]^{\mathrm{T}} \tag{55}$$

$$e_m(f_k) = \left[1, \ldots, e^{j2\pi (f_c + f_k)(M-1)\Delta\tau} \right]^{\mathrm{T}} \tag{56}$$

Thus, after transformation, the original form of

summation can be transformed into the following form.

$$\sum_{k=0}^{K-1}\frac{(2\pi f_k)^2|X(f_k)A(f_k)|^2}{\sigma_k^2} = \sum_{k=0}^{K-1}\frac{\boldsymbol{w}^{\mathrm{H}}\boldsymbol{\Sigma}_{XAE}(f_k)\boldsymbol{w}}{\boldsymbol{w}^{\mathrm{H}}\boldsymbol{\Sigma}_{NE}(f_k)\boldsymbol{w}} \tag{57}$$

Obviously, this problem is an optimization problem for multiple generalized Rayleigh quotient summations, which is caused by the unique structure of the TDL array. In the TDL structure, the delay line and phase shifter behind each antenna together form a frequency selective structure. When the frequency selection structures of multiple antennas are summed, the entire TDL matrix changes the SNR of the signals at different frequencies. Therefore, in the above summation, not only the signal term corresponding to the molecule is frequency-dependent, but also the noise term corresponding to the denominator is also frequency-dependent. Considering that the fractional summation problem is extremely difficult to handle, we amplify the noise term to simplify the problem, so there is

$$\begin{aligned}&\sum_{k=0}^{K-1}\frac{\boldsymbol{w}^{\mathrm{H}}\boldsymbol{\Sigma}_{XAE}(f_k)\boldsymbol{w}}{\boldsymbol{w}^{\mathrm{H}}\boldsymbol{\Sigma}_{NE}(f_k)\boldsymbol{w}}\\ &\le\sum_{k=0}^{K-1}\frac{\boldsymbol{w}^{\mathrm{H}}\boldsymbol{\Sigma}_{XAE}(f_k)\boldsymbol{w}}{\boldsymbol{w}^{\mathrm{H}}\boldsymbol{\Sigma}'_{NE}\boldsymbol{w}}\\ &=\frac{\boldsymbol{w}^{\mathrm{H}}\boldsymbol{\Sigma}'_{XAE}\boldsymbol{w}}{\boldsymbol{w}^{\mathrm{H}}\boldsymbol{\Sigma}'_{NE}\boldsymbol{w}}\end{aligned} \tag{58}$$

Our propose is to maximize the $\frac{\boldsymbol{w}^{\mathrm{H}}\boldsymbol{\Sigma}'_{XAE}\boldsymbol{w}}{\boldsymbol{w}^{\mathrm{H}}\boldsymbol{\Sigma}'_{NE}\boldsymbol{w}}$. However, the constant module optimization problem is a typical non-convex problem, it is difficult to directly obtain a closed-form solution, nor can it be solved directly by the convex optimization method. Therefore, we introduce a certain degree of relaxation in the processing process as shown in Ref.[41].

The constant modulus constraint problem is first relaxed into an inequality constraint problem in our paper. The original optimization problem can be written as:

$$\max_{\mathbf{w}}\frac{\boldsymbol{w}^{\mathrm{H}}\boldsymbol{\Sigma}'_{XAE}\boldsymbol{w}}{\boldsymbol{w}^{\mathrm{H}}\boldsymbol{\Sigma}'_{NE}\boldsymbol{w}} \tag{59}$$

$$\text{s.t.}\quad |\mathrm{w_i}|\le \mathrm{P_i}/\boldsymbol{D}_{ii} \tag{60}$$

Then the global optimal solution of this problem can be written as

$$\boldsymbol{w}=\eta\boldsymbol{v} \tag{61}$$

Among them, v is the main eigenvector of matrix ${\Sigma'_{NE}}^{-1}\Sigma'_{XAE}$, and η can be any value, for example, you can choose

$$\eta=\frac{1}{\left(\sqrt{\boldsymbol{D}_{kk}}\,|v_k|\right)/\sqrt{P_k}} \tag{62}$$

v_k represents the k-th element in the vector $\boldsymbol{v}$

$$k=\arg\max_{1\le i\le r}\frac{\boldsymbol{D}_{ii}\,|v_i|^2}{P_i} \tag{63}$$

For the equality constraints in the constant modulus optimization problem, the original optimization problem can be simplified as follows:

$$\begin{aligned}\max_{W}\quad &\frac{\boldsymbol{w}^{\mathrm{H}}\boldsymbol{\Sigma}'_{XAE}\boldsymbol{w}}{\boldsymbol{w}^{\mathrm{H}}\boldsymbol{\Sigma}'_{NE}\boldsymbol{w}}\\ \text{s.t.}\quad &|w_{m,n}|=1\end{aligned} \tag{64}$$

This problem is a typical generalized Rayleigh quotient problem if constant modulus constraints are not considered. Denote $\boldsymbol{u}$ as the primitive eigenvector of ${\boldsymbol{\Sigma}'_{NE}}^{-1/2}\boldsymbol{\Sigma}'_{XAE}{\boldsymbol{\Sigma}'_{NE}}^{-1/2}$,

$$\boldsymbol{w}^{opt}=\exp(\mathrm{j}\cdot\angle\boldsymbol{w}) \tag{65}$$

V. Numerical Simulation

In this section, we test the proposed algorithm by numerical simulation.

First, we verified the feasibility delay estimation under half-wave array conditions. The performances of the near CRLB estimation method are evaluated and compared with CRLB. Then, we verified that the TDL structure proposed in this paper can still work better than the traditional array. Similarly, the result is compared with the optimal pilot and the pseudo-random pilot. At last, the simulation shows that the optimal TDL matrix outperforms the DFT matrix, and the performance increases linearly with the number of antennas.

1. Estimation variance vs CRLB

Fig.1 shows the comparison of the estimation method presented in this paper with CRLB, in which the number of antennas of the antenna array is 16, 32, and 64, respectively. It can be found from the observation that in the case of a low SNR, the estimated variance given in this paper is inferior to CRLB; however, as the SNR rises to the range of –15 to –5dB, the performance of the

proposed method is close to CRLB. The reason is that as the SNR increases, the "arctan" function gradually shows a linearization trend. The conditions of the first-order Taylor expansion in the analysis gradually mature, and the phase estimation approximates the Gaussian distribution, which is consistent with the derivation process. As can be seen from the figure, as the number of antennas increases, the accuracy of delay estimation also increases.

What needs to be emphasized is that the received signal is under a relatively high SNR, because the core method proposed in this paper uses the first-order approximation. Therefore, we specifically analyze the impact of the received signal on the delay estimation when the SNR of the received signal is low. For this case, the phase estimation method in this manuscript will indeed deteriorate. It can be found from Fig.1 that for the case of low SNR, there is a large gap between the delay estimation performance of the phase method and the CRLB. The core of this phenomenon is because in a low SNR environment, the phase estimation performance of a single sampling point can no longer be approximated by the first-order linearization, and the approximation error is very large. However, we can still improve the estimation accuracy through some methods. First, for a low SNR environment, due to the use of a long pilot sequence, the traditional matched filtering method can be used to find the optimal estimation of the delay. At this time, the matched filtering process is realized through the FFT technology, which also searches for signal phase information on multiple frequency components. According to the analysis, the phase information on different frequency components of the signal has the law of linear change. The phase method provided in this article first calculates the phase of a single frequency point and then calculates the optimal delay estimate by the linear method. However, when the SNR is relatively low, the core of the traditional MLE method is to first combine the signal energies of multiple frequency points and then perform phase estimation. The essence of this estimation method makes use of the delay information contained in the signal phase, but by merging the signals, the SNR can be improved, and the problem of deterioration of the method in this paper under low SNR can be improved.

Meanwhile, it can be seen from Fig.1 that the accuracy of delay estimation increases after the number of antennas increases. For large-scale arrays, an increase in the number of antennas is intuitively manifested as an increase in the received signal power. According to the analysis of our manuscript, the CRLB of the delay estimation is positively correlated with the SNR. Therefore, with 64 antennas, more signal power can be obtained. In the optimal design proposed in this paper, the delay estimation result under 64 antennas is the best; while the delay estimation results for 32 antennas and 16 antennas decrease in order.

2. TDL structure vs traditional array

Fig.2 shows the comparison of the TDL structure proposed in this paper with the tradition. Compared with the traditional narrow-band array, the TDL array proposed in this paper has obvious advantages in the case of the number of antennas being 16, 32 and 64. What is particularly noticeable is that as the size of the antenna array increases, the delay estimation performance of the conventional array not only does not rise, but decreases, so that it is completely impossible under the conditions of large antenna size and high SNR. Meet the needs of the pass. This is because as the size of the antenna array increases, different antennas correspond to different data symbols, and only by phase-shifting the beat signals, the inter-code interference of the received signals is caused, and the SNR of the received signals is reduced and deteriorated. Estimate performance. Therefore, the traditional narrowband array can not only be used for the advantages of large-scale antenna arrays, but will be limited by its size, and the communication rate must be reduced. The TDL array has successfully solved this problem, making full use of the advantages brought by the increase in the size of the antenna array, and gradually reducing the estimation error.

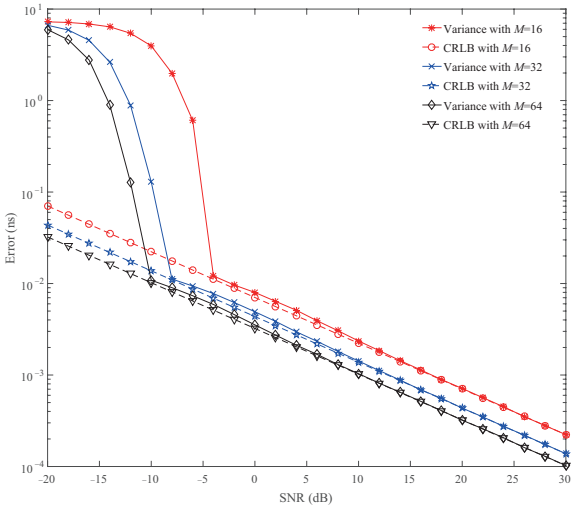

Fig. 1. Estimation variance vs CRLB under different numbers of antenna

3. Optimal training pilot

Fig.3 shows the synchronization performance comparison between the optimal training sequence and the traditional pseudo-random sequence proposed in this paper. When the number of antennas is 16, 32 and 64, the delay estimation accuracy of the optimal training sequence is much higher than that of the traditional pseudo-random sequence. This is because, in an actual communication system, the energy of the signal is mainly concentrated near the baseband zero frequency, such

as a typical sigma spectrum, and the high-frequency component is artificially suppressed. According to the discussion earlier in this paper, the high-frequency signal is more helpful to improve the accuracy of the delay estimation. Therefore, in this regard, the conventional pseudo-random pilot does not guarantee that the delay estimation error is the smallest. The training sequence design method proposed in this paper takes time delay estimation as the goal, rethinks the distribution of signal energy at each frequency point, and introduces the weighting coefficient $(2\pi f_k)^2$, consciously increases the proportion of high-frequency signals, and then in the constant envelope. The delay estimation performance of the signal is improved under constraints.

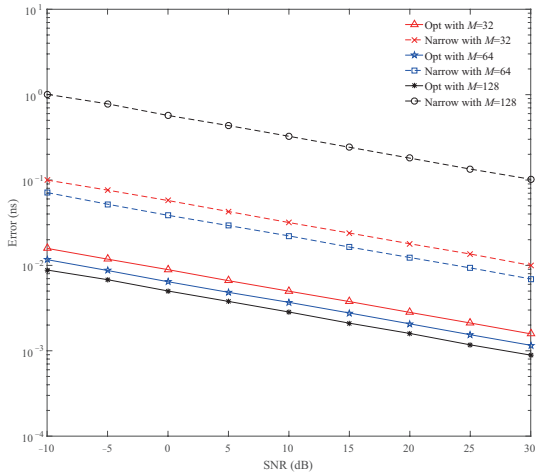

Fig. 2. TDL structure vs traditional narrowband array

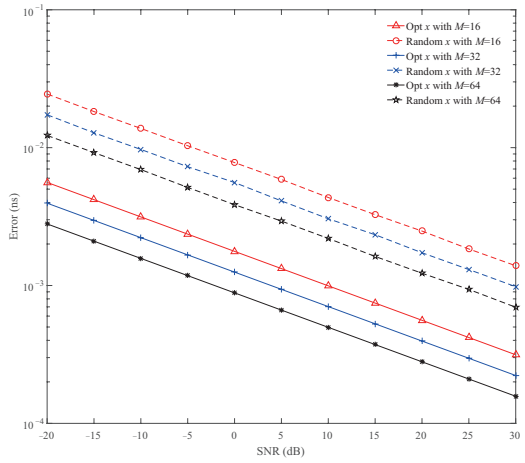

Fig. 3. Optimal training pilot vs pseudo-random pilot

4. Optiaml TDL matrix

Fig.4 and Fig.5 show the performance comparison between the optimal TDL array proposed in this paper and the traditional DFT-based TDL matrix.

Compared with the narrowband array structure, the DFT matrix-based TDL structure not only collects the signal energy of the center frequency point, but also collects the signal energy around the center frequency point, and thus the distortion due to excessive signal bandwidth. However, by comparison, it can be found that the optimal TDL matrix is superior to the DFT matrix in the case where the number of antennas is 16, 32, and 64, and in the case where the delayed series are sequentially 4, 6, and 8. Moreover, even with the TDL structure, the DFT matrix cannot solve the problem of reaching the asynchronous. Therefore, in the case where the number of antennas is relatively small, the DFT matrix can gradually improve the performance, but when the number of antennas is relatively large, the DFT matrix also has a performance deterioration problem. Moreover, the DFT matrix does not take full advantage of the advantages of the TDL architecture.

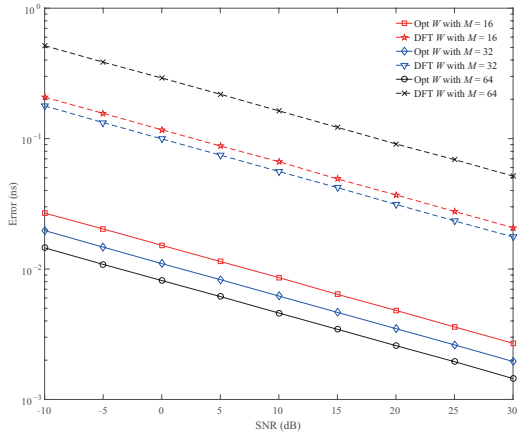

Fig. 4. Optiaml TDL matrix vs DFT matrix under different numbers of antennas

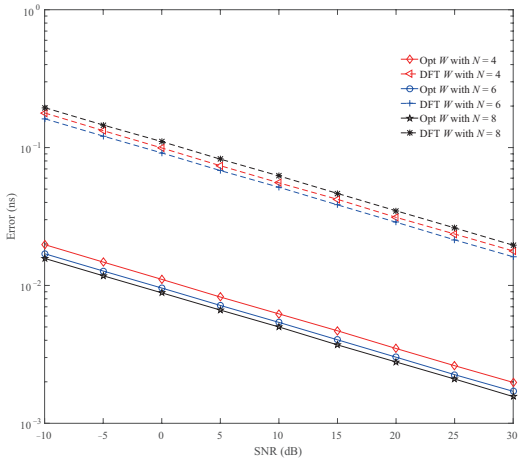

Fig. 5. Optiaml TDL matrix vs DFT matrix under different delay orders

As can be seen from Fig.4, for the TDL structure formed by the DFT matrix, the performance of 64 antennas is the best, and the performance of 16 antennas

exceeds 32 antennas. This is because for large-scale arrays, an increase in the number of antennas is intuitively manifested as an increase in the received signal power. According to the analysis of the article, the CRLB of the delay estimation is positively correlated with the SNR. Therefore, with 64 antennas, more signal power can be obtained. In the optimal design proposed in our article, the delay estimation result is the best; while the delay estimation results for 32 antennas and 16 antennas decrease in order. In contrast, for wide-band large-scale arrays, due to the increase in signal bandwidth, new influencing factors are introduced. For large-scale arrays, due to the sharp increase in the size of the array, the correlation of the received signals on each antenna is weakened, or even completely uncorrelated. Therefore, the use of a traditional DFT matrix for multi-antenna signal combination will suppress certain frequency components in the broadband signal and deteriorate the SNR of the received signal. In this way, the array gain no longer increases with the increase of the array size, and a larger-scale array destroys the received signal structure. Therefore, when the DFT array structure is adopted, it appears that the small-scale array has higher delay estimation accuracy.

Fig.6 shows the performance comparison of the optimal TDL matrix proposed in this paper under different delay levels.

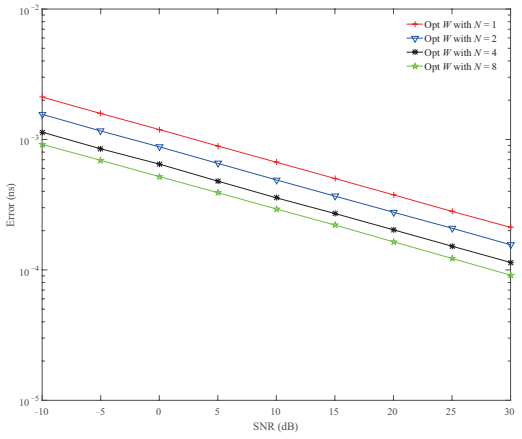

Fig. 6. Performance of optiaml TDL matrix under different delay orders

By comparison, the performance of the optimal TDL array is increasing with the increase of the delayed series. The performance improvement comes from two aspects. On the one hand, as the number of delay stages increases, the constant-mode TDL structure can approximate an ideal delay to achieve signal alignment on each antenna; on the other hand, as the number of delay stages increases The signal of a longer time enters the TDL structure, and the equivalent SNR is also improved, thereby improving the accuracy of the delay estimation.

IV. Conclusions

In this paper, we have proposed a new constant modulus TDL structure for the THz large-scale antenna array synchronization problem. Based on the proposed method, we have derived the CRLB for synchronous delay estimation and given a time delay estimation method that can gradually reach the CRLB. By minimizing the CRLB, the design method of optimal training sequence and the optimization method of optimal TDL matrix are given. Simulation results have shown that with the improvement of SNR, the proposed estimation method can quickly converge to reach the CRLB. Compared with the method of using the training pilot of the traditional pseudo-random sequence, the optimal pilot designed in this paper can achieve higher delay estimation accuracy. As the antenna size increases, the performance of the proposed TDL structure significantly exceeds the existing narrowband array structure. Furthermore, the performance of the optimal TDL matrix is also superior to that of the traditional DFT matrix-based structure.

References

[1] H. Sampath, P. Stoica and A. Paulraj, "Generalized linear precoder and decoder design for MIMO channels using the weighted MMSE criterion", *IEEE Transactions on Communications*, Vol.49, No.12, pp.2198–2206, 2001.

[2] D. P. Palomar, J. M. Cioffi and M. A. Lagunas, "Joint Tx–Rx beamforming design for multicarrier MIMO channels: A unified framework for convex optimization", *IEEE Transactions on Signal Processing*, Vol.51, No.9, pp.2381–2401, 2003.

[3] L. Li, D. Wang, X. Niu, Y. Chai, *et al.*, "mmWave communications for 5G: Implementation challenges and advances", *Science China* (*Information Sciences*), Vol.61, No.2, Article No.021301, 2018.

[4] H. Song and T. Nagatsuma. "Present and future of terahertz communications", *IEEE Transactions on Terahertz Science and Technology*, Vol.1, No.1, pp.256–263, 2011.

[5] T. Kleine–Ostmann and T. Nagatsuma, "A Review on Terahertz Communications Research, Journal of Infrared", *Millimeter and Terahertz Waves*, Vol.32, pp.143–171, 2011.

[6] C. Han, I. F. Akyildiz and W. H. Gerstacker, "Timing acquisition and error analysis for pulse-based terahertz band wireless systems", *IEEE Transactions on Vehicular Technology*, Vol.66, No.11, pp.10102–10113, 2017.

[7] Q. Liu, Y. Wang and A. E. Fathy, "A compact integrated 100Gs/s sampling module for UWB see through wall radar with fast refresh rate for dynamic real time imaging", *2012 IEEE Radio and Wireless Symposium, Santa Clara, CA*, pp.59–62, 2012.

[8] C. H. Sarantos and N. Dagli, "A photonic analog-to-digital converter based on an unbalanced Mach-Zehnder quantizer", *Optics Express*, Vol.18, No.14, pp.14 598–14 603, 2010.

[9] C. Han, A. O. Bicen and I. F. Akyildiz, "Multi-wideband waveform design for distance-adaptive wireless communications in the terahertz band", *IEEE Transactions on Signal Processing*, Vol.64, No.4, pp.910–922, 2016.

[10] B. Wang, F. Gao, S. Jin, *et al.*, "Spatial- and Frequency-wideband effects in millimeter-wave massive MIMO systems",

IEEE Transactions on Signal Processing, Vol.66, No.13, pp.3393–3406, 2018.

[11] M. Jian, F. Gao, Z. Tian, *et al.*, "Angle-domain aided UL/DL channel estimation for wideband mmWave massive MIMO systems with beam squint", *IEEE Transactions on Wireless Communication*, Vol.18, No.7, pp.3515–3527, 2019.

[12] R. Xin, Z. Ni, S. Wu, *et al.*, "Low-complexity joint channel estimation and symbol detection for OFDMA systems", *China Communications*, Vol.16, No.7, pp.49–60, 2019.

[13] M. M. U. Gul, X. Ma and S. Lee, "Timing and frequency synchronization for OFDM downlink transmissions using Zadoff-Chu sequences", *IEEE Transactions on Wireless Communications*, Vol.14, No.3, pp.1716–1729, 2015.

[14] S. B. Amor, S. Affes, F. Bellili, *et al.*, "Multi-node ML time and frequency synchronization for distributed MIMO-relay beamforming over time-varying flat-fading channels", *IEEE Transactions on Communications*, Vol.67, No.4, pp.2702–2715, 2019.

[15] R. Zhang, W. Xia, F. Yan, *et al.*, "A single–site positioning method based on TOA and DOA estimation using virtual stations in NLOS environment", *China Communications*, Vol.16, No.2, pp.146–159, 2019.

[16] R. Feng, Y. Liu, J. Huang, *et al.*, "Wireless channel parameter estimation algorithms: Recent advances and future challenges", *China Communications*, Vol.15, No.5, pp.211–228, 2018.

[17] X. Shen, Y. Liao, X. Dai, *et al.*, "Joint channel estimation and decoding design for 5G-enabled V2V channel", *China Communications*, Vol.15, No.7, pp.39–46, 2018.

[18] F. Cheng, G. Gui, N. Zhao, *et al.*, "UAV-relaying-assisted secure transmission with caching", *IEEE Transactions on Communications*, Vol.67, No.5, pp.3140–3153, 2019.

[19] N. Zhao, W. Lu, M. Sheng, *et al.*, "UAV-assisted emergency networks in disasters", *IEEE Wireless Communications*, Vol.26, No.1, pp.45–51, 2019.

[20] N. Zhao, X. Pang, Z. Li, *et al.*, "Joint trajectory and precoding optimization for UAV-assisted NOMA networks", *IEEE Transactions on Communications*, Vol.67, No.5, pp.3723–3735, 2019.

[21] Y. Gao, J. Xu and X. Jia, "Joint number and DOA estimation via the eigen–beam mCapon method for closely spaced sources", *Science China* (*Information Sciences*), Vol.58, No.12, pp.217–219, 2015.

[22] X. Xiong, Z. Deng, W. Qi, *et al.*, "High–precision angle estimation based on phase ambiguity resolution for high resolution radars", *Science China* (*Information Sciences*), Vol.62, No.4, pp.53–55, 2019.

[23] B. Rong, Z. Zhang, X. Zhao, *et al.*, "Robust superimposed training designs for MIMO relaying systems under general power constraints", *IEEE Access*, Vol.7, No.1, pp.80404–80420, 2019.

[24] Y. Ge, W. Zhang, F. Gao, *et al.*, "Angle-domain approach for parameter estimation in high-mobility OFDM with fully/partly calibrated massive ULA", *IEEE Transactions on Wireless Communications*, Vol.18, No.1, pp.591–607, 2019.

[25] S. Stein Ioushua, O. Yair, D. Cohen, *et al.*, "CaSCADE: Compressed carrier and DOA estimation", *IEEE Transactions on Signal Processing*, Vol.65, No.10, pp.2645–2658, 2017.

[26] P. Gupta and M. Agrawal, "Design and analysis of the sparse array for DoA estimation of noncircular signals", *IEEE Transactions on Signal Processing*, Vol.67, No.2, pp.460–473, 2019.

[27] B. Lin, J. Liu, M. Xie, *et al.*, "Direction-of-arrival tracking via low-rank plus sparse matrix decomposition", *IEEE Antennas and Wireless Propagation Letters*, Vol.14, pp.1302–1305, 2015.

[28] G. Qin, M. G. Amin and Y. D. Zhang, "DOA estimation exploiting sparse array motions", *IEEE Transactions on Signal Processing*, Vol.67, No.11, pp.3013–3027, 2019.

[29] M. Guo, Y. D. Zhang and T. Chen, "DOA estimation using compressed sparse array", *IEEE Transactions on Signal Processing*, Vol.66, No.15, pp.4133–4146, 2018.

[30] X. Yang, Y. Sun, T. Zeng, *et al.*, "Fast STAP method based on PAST with sparse constraint for airborne phased array radar", *IEEE Transactions on Signal Processing*, Vol.64, No.17, pp.4550–4561, 2016.

[31] O. Bar-Ilan and Y. C. Eldar, "Sub-Nyquist radar via Doppler focusing", *IEEE Transactions on Signal Processing*, Vol.62, No.7, pp.1796–1811, 2014.

[32] D. Cohen, D. Cohen, Y. C. Eldar, *et al.*, "SUMMeR: Sub-Nyquist MIMO radar", *IEEE Transactions on Signal Processing*, Vol.66, No.16, pp.4315–4330, 2018.

[33] K. Aberman and Y. C. Eldar, "Sub-Nyquist SAR via Fourier domain range-Doppler processing", *IEEE Transactions on Geoscience and Remote Sensing*, Vol.55, No.11, pp.6228–6244, 2017.

[34] L. Zheng and X. Wang, "Super-resolution delay-Doppler estimation for OFDM passive radar", *IEEE Transactions on Signal Processing*, Vol.65, No.9, pp.2197–2210, 2017.

[35] D. L. Donoho, A. Maleki, and A. Montanari, "Message passing algorithms for compressed sensing", *Proc. National Academy of Sciences*, Vol.106, pp.18914–18919, 2009.

[36] S. Rangan, "Generalized approximate message passing for estimation with random linear mixing", *arXiv:1010.5141*, 2010.

[37] M. Al-Shoukairi, P. Schniter and B. D. Rao, "A GAMP-based low complexity sparse Bayesian learning algorithm", *IEEE Transactions on Signal Processing*, Vol.66, No.2, pp.294–308, 2018.

[38] J. Vila and P. Schniter, "Expectation-maximization Bernoulli-Gaussian approximate message passing", *2011 Conference Record of the Forty Fifth Asilomar Conference on Signals, Systems and Computers* (*ASILOMAR*), Pacific Grove, CA, pp.799–803, 2011.

[39] C. Guo and J. D. B. Nelson, "Direction of arrival estimation via approximate message passing", *2nd IET International Conference on Intelligent Signal Processing 2015* (*ISP*), London, pp.1–6, 2015.

[40] C. Wei, H. Liu, Z. Zhang, *et al.*, "Approximate message passing-based joint user activity and data detection for NOMA", *IEEE Communications Letters*, Vol.21, No.3, pp.640–643, 2017.

[41] V. Havary-Nassab, S. Shahbazpanahi, A. Grami, *et al.*, "Distributed beamforming for relay networks based on second-order statistics of the channel state information", *IEEE Transactions on Signal Processing*, Vol.21, No.3, pp.640–643, 2017.

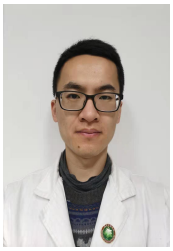

ZHENG Chen was born in 1988. He received the B.S. degree in electronic information and communication from Beijing Institute of technology. He is a Ph.D. candidate of information and communication engineering. His research interests include wireless communication and massive MIMO.
(Email: mz3721@126.com)

DING Xuhui (corresponding author) received the B.S. degree from Beijing Institute of Technology in 2014, and is currently pursuing the Ph.D. degree with the Beijing Institute of Technology, Beijing, China. His research interests include high data rate wireless communication, channel coding, iterative detection, massive MIMO systems, and Terahertz communication. (Email: dxh387@163.com)

LIU Dekang was born in 1990. He received the B.S. and Ph.D. degrees in information and communication engineering from Beijing Institute of technology. His research interests include signal processing, massive MIMO systems, high frequency band communication systems, and convex optimization. (Email: dkliu17@126.com)

BU Xiangyuan received the B.E. and Ph.D. degrees from Beijing Institute of Technology, Beijing, China, in 1987 and 2007, respectively. From 1996 to 1998, he was a visiting scholar at the Military Academy of Belarus, Belarus. Since 2002, he has been with the School of Information and Electronics, BIT, where he is currently a Professor. His current research interests include wireless communication, digital signal processing, and channel coding. (Email: bxy@bit.edu.cn)

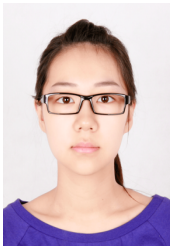

AN Sining received the B.S. and M.S. degrees in communication and electronics engineering from the Beijing Institute of Technology, Beijing, China, in 2013 and 2016. She is currently a Ph.D. student in the Microwave Electronics Laboratory, Department of Microtechnology and Nanoscience, Chalmers University of Technology. Her research interests include high data rate communication, modulation and demodulation and high-resolution radar. (Email: sininga@chalmers.se)